Quasiconformal Maps in Transformation Optics and Their Electrostatic Analogs

Fu Liu[1], Pengjiang Wei[2], Z. Chang[3], Gengkai Hu[3] and Jensen Li[1,4]
[1]School of Physics and Astronomy, University of Birmingham, Birmingham B152TT, United Kingdom
[2]Department of Physics and Materials Science, City University of Hong Kong, Tat Chee Avenue, Kowloon, Hong Kong
[3]School of Aerospace Engineering, Beijing Institute of Technology, Beijing 100081, P. R. China
[4]Shenzhen Research Institute, City University of Hong Kong, Shenzhen, P. R. China

***Abstract*- Quasiconformal maps have been utilized for generating transformation optical devices with a range of applications including invisibility cloaks, waveguide benders, couplers, surface-conformal lenses and antennas. Here, we discuss their generation by numerically solving the Poisson's equation where the analytic solution of a typical electrostatic problem in the virtual space acts as a seed in numerically generating a quasiconformal map with a transformed shape of boundary. Two examples about capacitor under external voltage and a point charge in a cavity are given.**

I. Introduction

Transformation optics has been becoming an emerging technique in designing optical devices [1]-[3]. It provides an intuitive method in designing optical devices by using a coordinate transformation. A coordinate transformation keeps the Maxwell's equations form-invariant with an induced transformation on the electric permittivity and magnetic permeability. By realizing the induced material profile using metamaterials, the resultant optical device thus provides the same function to the one before transformation. This functional equivalence provides an effective route to change the size and the shape of an object. The most prominent example is an invisibility cloak to diminish the size of an object [2]-[16]. In fact, the coordinate transformation is quite arbitrary and it becomes a well-posed engineering task to choose the optimal one so that the induced material parameters can be constructed and fabricated using metamaterials easily. One such attempt is the quasiconformal map which can minimize the maximum anisotropy in the induced materials profile in which the anisotropy of available materials for construction is limited for specific examples [5]. This facilitated the realization of dielectric cloaks at optical frequencies and has been used to design a range of transformation optical devices including waveguide benders, couplers and antennas [17]-[22]. A quasiconformal map can be regarded as a generalized variant of a conformal map with an additional advantage that the boundary of the transformed region, i.e. the size and shape of the transformation optical device, can be predefined. This gives rise to a small constant anisotropy, due to a general difference in conformal module before and after transformation, which can be further neglected as an approximation so that only isotropic materials are needed for realization. While for a conformal map, a finite size of transformation optical device can be obtained by a cutoff in dielectric constant as a similar approximation. We can also use a quasiconformal map to approach a conformal map if the shape of the virtual domain in specific applications can be changed so that the conformal module matches before and after transformation [23].

This paper presents a straightforward two-steps design in generating a quasiconformal map using electrostatic analogy. First, we start with an electrostatic problem with analytic solution in the virtual space. Second, by numerically solving the same electrostatic problem (Poisson's equation) with a transformed boundary of the analytic problem in the physical space, we generate the numerical quasiconformal map. Finally, full wave simulations are used to demonstrate the function of the resultant transformation optical devices with the generated quasiconformal maps.

II. Electrostatic analogs in generating Quasiconformal maps

In this paper, we only focus on two dimensional transformation optical devices. We start with a map which transforms a rectangle (e.g. a vacuum) with coordinates $0 \le \xi \le w$ and $0 \le \eta \le h$ to a general quadrilateral with curved boundaries. By considering all possible coordinate transformations which map the 4 corners of the rectangle to the 4 corners of the curved quadrilateral and the 4 edges of the rectangle to the 4 edges of the curved quadrilateral with sense preserved but no further restrictions, one can prove the map generating the minimal of maximum anisotropy in the whole medium minimizes the Modified Liao functional [5]:

$$\Phi = \int_0^w d\xi \int_0^h d\eta \frac{Tr(g)^2}{\det g}. \quad (1)$$

Such a functional minimization can then be equivalent to solving [24]

$$\begin{aligned} \frac{\partial^2 \xi}{\partial x^2} + \frac{\partial^2 \xi}{\partial y^2} &= 0, \\ \frac{\partial^2 \eta}{\partial x^2} + \frac{\partial^2 \eta}{\partial y^2} &= 0. \end{aligned} \quad (2)$$

subject to the same boundary conditions. In fact, the resultant map is the quasiconformal map which is a type of orthogonal maps. It has two implications. One is that we can just use the Dirichlet-Neumann boundary condition [24] (Dirichlet boundary for ξ and Neumann boundary for η or vice versa). The quasiconformal map transforms a tiny square in the (ξ, η)

978-1-4799-6281-5/15/$31.00 ©2015 IEEE

coordinates to a tiny rectangle in the (x, y) coordinates with constant aspect ratio $\alpha = \partial_y\eta/\partial_x\xi = -\partial_x\eta/\partial_y\xi$. Suppose we are working in the transverse-electric (E_z) polarization. The transformed medium in the (x, y) coordinates has the permittivity profile (with respect to the medium in (ξ, η) coordinates) as

$$\epsilon_z = |\nabla\xi|^2\alpha = |\nabla\eta|^2/\alpha \quad (3)$$

and a permeability (tensor on the x-y plane) profile with the ratio between the two principal values as constant α^2. The anisotropy of the quasiconformal map is minimized (maximum of $\alpha + 1/\alpha$ is minimized). If α is sufficiently near to the value one, we then only realize Eq. (3) and neglect the permeability tensor. Another implication is that we can have an electrostatic analog towards Eq. (2) and it can be used to construct a composite map. In this case, the quasiconformal map is used as a tool for designing generic optical devices (not necessarily minimizing anisotropy). The potential V corresponds to ξ while the streamlines of electric field $\boldsymbol{E}$, surface normal to the equipotential contours, corresponds to the constant-η lines or vice versa. Suppose we know the analytic solution of a typical electrostatic problem in solving Eq. (2) with coordinates (x', y') (instead of x and y). For example, it can be a parallel plate capacitor under an applied voltage, or a point source within a grounded circular cavity, shown in the left hand side of Fig. 1. On the other hand, we numerically solve the same problem in the physical coordinates (x, y) with deformed shape of boundaries (right hand side of Fig. 1). Then, the transformation from the virtual to physical space is a composite map ($(x', y') \leftrightarrow (\xi, \eta) \leftrightarrow (x, y)$).For simplicity, we assume the first map is conformal and the overall transformation induces a permittivity profile as

$$\epsilon_z = \frac{|\nabla\xi|^2\alpha}{|\nabla'\xi|^2} = \frac{|\nabla\eta|^2/\alpha}{|\nabla'\eta|^2}. \quad (4)$$

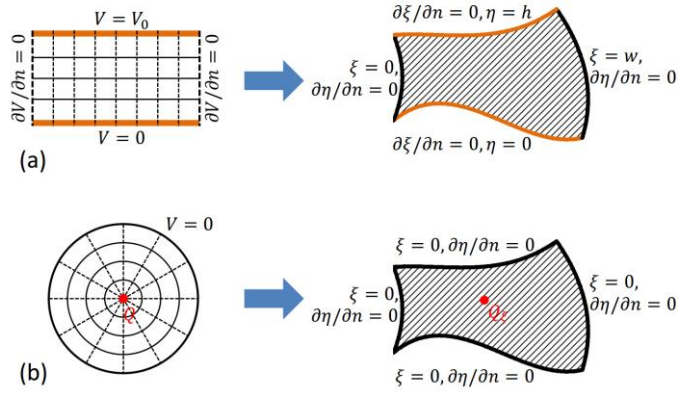

Fig. 1 Electrostatic analog as a starting point in generating a quasiconformal map on the right with deformed boundaries. (a) A capacitor under an applied voltage with η acting as the voltage. Contours of constant ξ acts as the E-field stream lines. (b) A point charge within a gounded cavity. The size of the point charge controls the resultant anisotropy α. Contours of constant-ξ/η aligns with constant-V lines /E-field streamlines.

III. Numerical examples

As the first example, we consider a parallel plate capacitor (Fig. 1(a)) as a trivial example. A starting analytic solution (interpreting η as electrostatic potential) can be taken as $\eta = y'$ while the orthogonal coordinate (assumed conformal) can be taken as $\xi = x'$. Next, we numerically solve the same system but with deformed bottom boundary (Fig. 2(a) for solving ξ and 2(b) for solving η with the specified Dirichlet-Neumann boundary conditions) in generating the quasiconformal map. The permittivity, according to Eq. (4), is plotted in Fig. 2(c). Such a permittivity profile can be used as a carpet cloak on top of a reflecting bump. Full-wave simulation with E_z polarization for an incident beam at an incident angle of 45 degrees has been performed and the resultant E-field profile is shown in Fig. 2(d). It agrees with the results in Ref. [5], showing scattering cancellation. Furthermore, the electrostatic analog interpretation gives us the extra flexibility in designing transformation optical devices by choosing other kinds of electrostatic analogs.

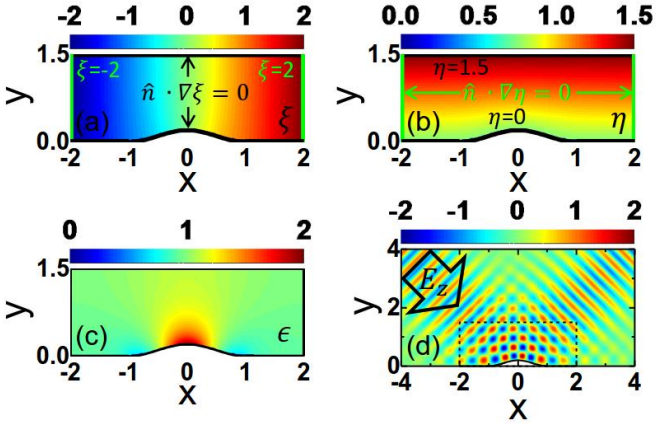

Fig. 2 Carpet cloak. (a),(b): ξ and η profile in the physical space by solving Eq. (2) with the specified Dirichlet-Neumann boundary conditions; (c): induced permittivity; (d) Full-wave simulation for an incident beam at 45 degrees.

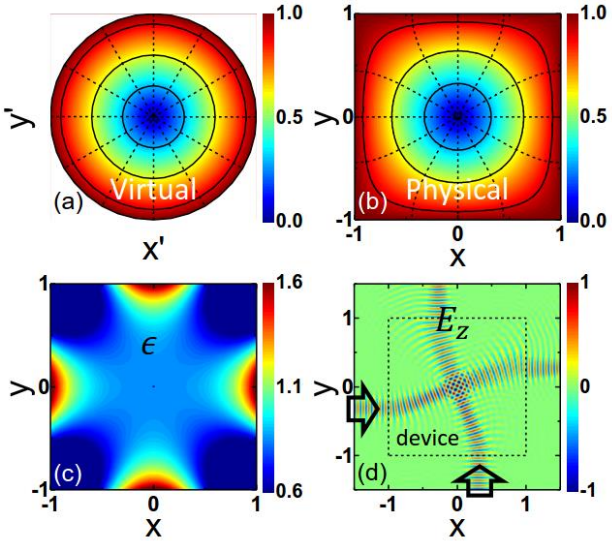

Fig. 3 Double shifter. (a) Virtual space with. r'-contours (analogs of equipotential contours for a point charge at origin) in concentric circles. ϕ'-contours in radial lines. (b) Physical

space with the corresponding contour lines. (c) induced permittivity; (d) Full-wave simulation with incident beams from bottom and left.

Next, we consider another electrostatic problem of a point charge at the center of a circular grounded cavity of radius 1 (Fig. (b)) to design a shifter in both x and y-direction . A starting analytic solution (interpreting ξ as electrostatic potential V for the point source) can be taken as $\xi = \ln(r') = \ln\sqrt{x'^2 + y'^2}$ and its orthogonal coordinate $\eta = \phi' = \arg(x' + iy')$ where $\xi \in (-\infty, 0]$ and $\eta \in [0,2\pi)$. Next, we numerically solve the same problem (a point charge) in the physical space with square boundary (Eq. (2)) with Dirichlet-Neumann boundary conditions ($\xi = 0$ and $\partial_n \eta = 0$). Fig. 3(a) and 3(b) show the resultant r' and ϕ'-contours in the virtual and physical space respectively. The induced permittivity profile is shown in Fig. 3(c). As ξ goes to infinity at the point charge, the size of the point charge in the physical space gives us an additional flexibity to control the resultant anisotropy. Figure 3(d) shows the full-wave simulation when there are both incident beams from bottom and from the left. As the circular boundary in the virtual space is now flattened, the incident beams now appear shifted by travelling alng the ϕ'-contours.

IV. Conclusion

By solving a typical electrostatic problem (Poisson's equation) in the virtual space with analytic solution and numerically solving the same problem in the physical space with deformed boundaries, we have established a generic way for generating quasiconformal maps from the virtual to the physical space by employing different electrostatic analogs (with permittivity obtained from Eq. (4) by taking ξ or η as analog of potential V). It gives addition flexibility in designing transformation optical devices enabled by quasiconformal maps.

ACKNOWLEDGMENT

The work is supported by the National Natural Science Foundation of China (grant no. 11104235) from the Shenzhen Research Institute, City University of Hong Kong.

REFERENCES

[1] J. B. Pendry, A. J. Holden, D. J. Robbins, and W. J. Stewart, *IEEE Trans. Micr. Theory and Techniques*, 47, 2075 (1999).
[2] J. B. Pendry, D. Schurig, and D. R. Smith, *Science* **312** 1780 (2006).
[3] U. Leonhardt, *Science* **312** 1777 (2006).
[4] D. Schurig et.al., *Science,* **314,** 977-80 (2006).
[5] J. Li and J. B. Pendry, Phys. Rev. Lett. 101,203910 (2008).
[6] R. Liu, et al. Science 32, 366-369 (2009).
[7] U. Leonhardt and T. Tyc, Science 323, 110 (2009).
[8] J. Valentine, J. Li, T. Zentgraf, G. Bartal, X. Zhang, Nat Mater 8, 568 (2009).
[9] L. H. Gabrielli, J. Cardenas, C. B. Poitras, M. Lipson, Nat Photon 3, 461–463 (2009).
[10] T. Ergin et.al., Science 328, 337–339 (2010).
[11] H. F. Ma and T. J. Cui, Nat Commun 1, 1–6 (2010).
[12] F. Zhou et.al., Nat. Sci. Rep. 1 78 (2011).
[13] M. Gharghi, C. Gladden, T. Zentgraf, Y. Liu, X. Yin, J. Valentine and X. Zhang, Nano Lett. 11 2825−8 (2011).
[14] X. Chen et.al., Nature Comm. 2, 176 (2011).
[15] B. Zhang et.al., Phys. Rev. Lett. 106,033901 (2011).
[16] N. Landy and D. R. Smith, Nature Mater. 12, 25 (2013).
[17] N. I. Landy, N. Kundtz, D. R. Smith, Phys. Rev. Lett. 105, 193902 (2010).
[18] Z. L. Mei, J. Bai and T. J. Cui, New. J. Phys. 13, 063028 (2011).
[19] R. Yang, W. Tang and Y, Hao, Opt. Exp. 19, 12348 (2011).
[20] C. Garcia-Meca, A. Martinez and U. Leonhardt, Opt. Exp. 19, 23743 (2011).
[21] L. H. Gabrielli, D. Liu, S. G. Johnson and M. Lipson, Nature Comm. 3, 1217 (2012).
[22] Q. Wu, J. P. Turpin and D. H. Werner, Light: Science & Applications 1, e38 (2012).
[23] N. I. Landy and W. J. Padilla, Opt. Exp. 17, 14872 (2009).
[24] Z. Chang, X. Zhou, J. Hu and G. K. Hu, Opt. Exp. 18, 6089 (2010).
[25] T. Zentgraf et.al., Adv. Mater. 22, 2561 (2010).